The Linnean Society of London
ZOOLOGICAL Journal of the Linnean Society

Towards the identification of the ommastrephid squid paralarvae (Mollusca: Cephalopoda): morphological description of three species and a key to the Northeast Atlantic species

Journal:	*Zoological Journal of the Linnean Society*
Manuscript ID	ZOJ-03-2016-2516.R2
Manuscript Type:	Original Article
Keywords:	morphological comparison < Anatomy, morphology < Anatomy, larvae < Development, North Atlantic < Geography, Mollusca < Taxa, Cephalopoda, identification key < Taxonomy, intraspecific variation < Taxonomy

Abstract

Oceanic squids of the family Ommastrephidae are an important fishing resource worldwide. Although cumulative knowledge exists on their subadult and adult forms, little is known about their young stages. Their hatchlings are among the smaller cephalopod paralarvae. They are characterized by the fusion of their tentacles into a proboscis and are very difficult to identify to species level, especially in areas where more than one species coexist. Seven species are found in the NE Atlantic. In this study, mature oocytes of *Illex coindetii*, *Todarodes sagittatus* and *Todaropsis eblanae* were fertilized *in vitro* to obtain and describe hatchlings. Full descriptions based on morphometric characters, chromatophore patterns, skin sculpture, and the structure of proboscis suckers are provided based on live specimens. This information was combined with previous descriptions of paralarvae, not necessarily based on DNA or known parentage, from four other ommastrephid species distributed in the same area and a dichotomous key was developed for the identification of paralarvae of the NE Atlantic. The most useful taxonomic characters were: the relative size of the lateral and medial suckers of the proboscis, the presence/absence of photophores, and the arrangement of pegs on the proboscis suckers. This key was successfully used to identify wild collected rhynchoteuthion paralarvae from the NE Atlantic. Reliable identification of wild paralarvae can foster a better understanding of the population dynamics and life cycles of ommastrephid squids.

Keywords: Morphology, NE Atlantic, Mediterranean Sea, marine taxonomy, *in vitro* fertilization, Scanning Electron Microscopy.

Introduction

Ommastrephid squids are distributed in all the world´s oceans and their rapid growth and abundance make them the most important cephalopod fishery resource (Arkhipkin et al., 2015). Knowledge of early life stages is essential for understanding ecology and life cycles as well as for assessment of fisheries. These oceanic squids are important prey and predators, occupying a wide range of trophic levels in marine pelagic food webs (Coll et al., 2013). They are also dominant prey in the diet of many top fish predators (Logan et al., 2013) as well as seabirds and marine mammals (Boyle & Rodhouse, 2005). Despite the cumulative knowledge on the biology of subadult and adult forms of several species of this family, present knowledge of early life stages is fragmentary and limited. Hatchlings of this family are among the smaller of the cephalopods and show a characteristic morphology with tentacles fused into a proboscis. These paralarvae are known as rhynchoteuthion. Identification of the early stages of several species is considerably difficult (Nesis, 1979; Sweeney et al., 1992), especially in areas where more than one species coexists (Gilly et al., 2006; Ramos-Castillejos et al., 2010). Based on wild-collected ommastrephid planktonic stages from around the world, Nesis (1979) stated that it is possible to identify rhynchoteuthion paralarvae to genus, but not species level. Nine of the 22 accepted ommastrephid species (Jereb & Roper, 2010) occur in the N Atlantic Ocean. In the NE Atlantic Ocean, seven ommastrephid species can be found: *Illex coindetii* (Verany, 1839), *Todaropsis eblanae* (Ball, 1841), *Todarodes sagittatus* (Lamarck, 1798), *Ommastrephes bartramii* (Lesueur, 1821), *Sthenoteuthis pteropus* (Steenstrup, 1855), *Hyaloteuthis pelagica* (Bosc, 1802) and *Ornithoteuthis antillarum* Adam, 1957. Besides these, *I. illecebrosus* (Lesueur, 1821) and *I. oxygonius* Roper, Lu & Mangold, 1969 occur in the NW Atlantic. Previous works have dealt with the morphology of the paralarvae of *I. illecebrosus* (e. g. Roper & Lu, 1979; O´Dor et al., 1982). However, the taxonomic status of the NW Atlantic *Illex* spp. populations and the extent of their distribution range are not resolved. Even adult individuals are difficult to identify by morphological characters when more than one species occurs (Carlini, Kunkle & Vecchione, 2006). Thus, NW *I. illecebrosus* and *I. oxygonius* were not included in this work.

The rhynchoteuthion paralarvae of *O. bartramii* (Young & Hirota, 1990; Watanabe et al., 1996; Vijai, Sakai & Sakurai (2015) and *I. coindetii* (Boletzky, Rowe & Aroles, 1973; Villanueva et al., 2011) have been studied from hatchlings obtained during laboratory experiments. The morphology of *O. bartramii* paralarvae from the NW Pacific was studied from *in vitro* fertilizations (Watanabe et al., 1996; Vijai et al., 2015) and the morphology of some paralarvae collected in the wild assigned to this species (Young & Hirota, 1990) is consistent with the chromatophore pattern reported in both types of studies. Only descriptions of *H. pelagica*, *O. antillarum* and *S. pteropus* paralarvae collected in the wild are available (Harman & Young, 1985; Sweeney et al., 1992). Nesis (1979) provided a description of wild-collected individuals of *T. sagittatus*, *T. angolensis* Adam, 1962 and *T. pacificus* (Steenstrup, 1880). However, he merged the characters of the three species into a single generic description and the specific characters of *T. sagittatus* are not available. For *I. coindetii*, complete descriptions of the morphology and chromatophore pattern of the paralarvae are lacking. Moreover, the hatchlings of *T. eblanae* are undescribed. The current situation makes species identification of wild rhynchoteuthion paralarvae from the NE Atlantic nearly impossible using morphological characters (e. g. Zaragoza et al., 2015). This strongly limits the study of the ecology and biology of rhynchoteuthions from the NE Atlantic (e.g. Moreno et al., 2009).

In order to address this problem, we used *in vitro* fertilization methods to obtain live paralarvae of the three most fished NE Atlantic ommastrephid species (*I. coindetii*, *T. sagittatus* and *T.*

eblanae) and provide detailed descriptions of their morphology and chromatophore pattern. The available knowledge on the morphology of rhynchoteuthions of the other four NE Atlantic species (*O. bartramii*, *S. pteropus*, *H. pelagica* and *O. antillarum*) was reviewed from the literature. Moreover, a key for the identification of the ommastrephid paralarvae from the NE Atlantic is also provided, aiming to offer a tool for the study of the biology and population dynamics of paralarval stages of ommastrephid squids.

Material and methods

Obtaining paralarvae through in vitro *fertilizations*

Adult squids of *I. coindetii*, *T. sagittatus* and *T. eblanae* were captured by local bottom trawlers from Barcelona and Vilanova i la Geltrú, NW Mediterranean Sea, between May 2010 and April 2015. *Illex coindetii* and *T. eblanae* were captured from 120 to 350 m depth, and *T. sagittatus* from 300 and 400 m depth. Special care was taken in selecting the freshest squids captured during the latest trawl of the day. Selected individuals were placed on crushed ice covered by a plastic film and transported to the laboratory. Mature females with oocytes in oviducts (stage V-VI according to Brunetti, 1990) were selected for *in vitro* fertilizations following the general methodology described by Villanueva et al. (2012) with minor modifications. In short, for *I. coindetti*, the sperm source used was the bulbs of spermatangia attached to the internal mantle of the female; for *T. eblanae* spermatophores of the Needham´s sac and the *vas deferens* from male individuals were used; for *T. sagittatus*, sperm from spermatophores or seminal receptacles and spermatangia was used depending on availability. The oviducal glands used to make the oviducal jelly were obtained from mature females of the same species collected previously. Freeze-dried oviducal gland powder was stored at -80ºC until use. The fertilization percentage of each female used during the experiments was estimated one day after fertilization, by counting the number of fertilized eggs from a sample of 400-500 eggs (Table S1). When more than one female was used in an experiment, the mean fertilization rate of the experiment was calculated and is indicated in Table S1. Sterile 60-mm diameter polystyrene Petri dishes each containing 20-50 fertilized eggs were maintained in the dark at 15, 17 or 21 ºC using incubators (see Table S1). Since vertical distribution of egg masses of the species studied is unknown, temperature conditions during natural embryonic development remain uncertain. Therefore, the temperatures chosen for egg incubation in the present study were based on the temperature ranges of mid-water layers in the Mediterranean Sea (Brasseur et al., 1996), where the egg masses are expected to occur. Throughout the experiment, 25 mg l^{-1} of two antibiotics, ampicillin and streptomycin, were added to the filtered seawater (FSW) (Staaf et al., 2008). The FSW with antibiotics was replaced daily using a binocular microscope and sterile plastic pipettes. Dead embryos and those with abnormalities were removed and counted daily to determine the survival rates until the hatchling stage.

In all the experiments, the paralarvae were cared for and euthanized with the ethical methods in accordance with the European Union Directive 2010/63/EU. Paralarvae were anaesthetized adding drops of 70% ethanol to Petri dishes containing approximately 12 ml of FSW and overdoses of anaesthesia were used to euthanize them. The initial stages of anaesthesia started very gradually, adding only a few drops of ethanol to the Petri dish containing the paralarvae over a period of 15-30 min, aiming to avoid signals of irritation such as body contractions or ink ejection.

Observations of live paralarvae

For accurate classification of embryonic stages, the scheme and definitions published for *Illex argentinus* (Castellanos, 1960) (Sakai et al., 1998) and *Todarodes pacificus* (Watanabe et al., 1996) were directly applied to *I. coindetii* and *T. sagittatus*, respectively. The *T. pacificus* scale was also adapted for *T. eblanae*. To avoid confusion between supposedly premature hatched individuals and the expected normal hatching, hatchlings are defined here as individuals with a well-developed ink sac, extensible proboscis and functional fins with a fin width nearly equal to the head width. These developmental criteria can be found at stage XXX for the genus *Illex* (Sakai et al., 1998; Villanueva et al., 2011) and stage XXXII for *Todarodes* and *Todaropsis* (see Discussion). The descriptions were based on individuals of these stages.

The morphological description was based on measurements of several morphometric characters. These measures were defined according to Roper & Voss (1983) as the ventral mantle length (VML), the dorsal mantle length (DML), the total length (TL), the head length (HL), the head width (HW), the eye diameter (ED), the funnel length (FuL), and the length of the second pair of arms (AIIL). Two other characters were added to the morphometric descriptions. Since the proboscis length was observed to change according to its contraction state, the total length without the proboscis (TL w P) was also measured and was defined as the length of the paralarva from the posterior tip of the mantle to the tip of the arm I. The proboscis width at the base (PW) was defined as the maximum width of the proboscis at its base. The proboscis length has been used as a taxonomic character (e. g. Diekmann, Piatkowski & Schneider, 2002). However, this character varies highly with contraction state (Nesis, 1979; Sweeney et al., 1992; Staaf et al., 2008) and usually changes throughout the ontogeny (Shea, 2005). Harman & Young (1985) provided the proboscis length and the proboscis index of *Nototodarus hawaiiensis* (Berry, 1912), *H. pelagica* and *Sthenoteuthis oualaniensis* (Lesson, 1830-1831). Although they considered *N. hawaiiensis* to have a "typically short" proboscis and *S. oualaniensis* often with a "very elongate" proboscis, both the proboscis length (Harman & Young, 1985: Fig. 2) and their proboscis index overlap. Both characters also overlap with *H. pelagica*, as confirmed in other posterior references (Sweeney et al., 1992; Diekmann et al., 2002). Thus, this character is not very instructive and was not considered in our study. When resting on the Petri dishes, the majority of the embryos or paralarvae lay on the dorsal surface of the body; thus, it was not possible to measure the DML in many specimens. For this reason, the ratio between each morphometric parameter and body size was obtained using the VML instead of the DML. The terminology used for discriminating rhynchoteuthion types was: Type A, the ratio of sucker sizes is greater than 2:1 (lateral suckers 200% or greater in size than the medial suckers), Type B, this ratio is between 1.1:1 and 1.9:1 (lateral suckers larger than the medial suckers but below 200%) and Type C, this ratio is 1:1 (there is no size difference among the proboscis suckers). These three categories are consistent with the proboscis sucker proportions of ommastrephid paralarvae A, B, and C treated in Roper & Lu (1979).

For the description of the chromatophore pattern, the dorsal and ventral surfaces were depicted in a schematic drawing of a rhynchoteuthion. Lateral views were only considered for the description when hatchling chromatophores were visible only from the side view. For *I. coindetii* and *T. sagittatus*, the lateral view was not included, since the lateral chromatophore pattern is the sum of the dorsolateral and ventrolateral chromatophores. However, *T. eblanae* has true lateral chromatophores in the midline of the lateral surface of the mantle, which are not visible from dorsal or ventral views. The chromatophores of the head and mantle were assigned to rows in an anteroposterior axis. For example, for the ventral mantle, the pattern 4 + 2 + 3 + 4 + 1 + 2 means: 4 chromatophores in the anterior margin of the mantle, 2 in the second row, 3 in

the third row, 4 in the fourth row, 1 in the fifth row and 2 near the posterior tip of the mantle. The mode of the pattern of each row was considered the most representative of the species and a schematic drawing depicting this pattern is provided for each species.

Observations under scanning electron microscopy (SEM)

Paralarvae were euthanized with an overdose of anaesthesia prior to fixation. To avoid body contraction of the paralarvae it is important to add the anaesthetic gradually before killing them, starting anaesthesia with a few drops of ethanol. Once the three hearts stopped beating, the individuals were fixed in 2.5% glutaraldehyde in seawater for 24-48 h, washed in seawater followed by dehydration in an increasing concentration of ethanol (20, 30 and 50%) and stored in 70% ethanol in the dark at 4 °C. At the beginning of SEM preparation, the samples were again dehydrated in an increasing concentration of ethanol (80, 90, and 96%) until they were saturated in absolute ethanol. Each ethanol bath lasted 10 min. After complete dehydration in the ethanol series, the samples were dried to a critical point using CO_2 as the transition liquid. After the drying stage, samples were mounted on stubs with double-sided conductive sticky tape to place them in the preferred position. The mounted samples were sputter coated with gold–palladium. Finally, the samples were observed using a scanning electron microscope.

The general morphology and the number and arrangement of pegs in the proboscis and arm suckers were examined. Nomenclature of proboscis suckers was as follows. The suckers were named from 1 to 4 of each hemiproboscis tip, with 1 the most dorsal and 4 the most ventral. Each side of the proboscis tip was named as R (right) or L (left), according to its position on the anteroposterior axis of the body. For example: proboscis sucker R1 is the most dorsal sucker from the right part of the proboscis tip. Suckers 2 corresponded to lateral suckers and suckers 1, 3 and 4 were medial suckers. Newly hatched rhynchoteuthion paralarvae only have one sucker on arms I and II. Thus, no special nomenclature was necessary to designate each sucker.

Characters from both SEM and observations of live paralarvae were used to develop a dichotomous key to facilitate the identification of the seven NE Atlantic rhynchoteuthion paralarvae species. Morphological characters of *O. bartramii, H. pelagica*, *S. pteropus* and *O. antillarum* were obtained from the literature (Harman & Young, 1985; Sweeney et al., 1992; Young & Hirota, 1990; Sakurai et al., 1995; Diekmann et al., 2002; Vijai et al., 2015). It should be noted that descriptions of the paralarvae of *H. pelagica*, *S. pteropus* and *O. antillarum* were not confirmed by DNA or known parentage in these works.

Wild rhynchoteuthion paralarvae samples

Wild rhynchoteuthion paralarvae (n = 16) from the study area were collected using zooplankton tows during the oceanic cruise LLUÇ3 (Palomera, Olivar & Morales-Nin, 2005) in the summer of 1999, NW Mediterranean; four oceanographic cruises conducted in the summers of 2003 and 2004 under the CACO research project (Sabatés et al., 2009), NW Mediterranean; and another cruise near the Canary Islands in the spring of 2015 under the MAFIA research project using the fishing net described by Meillat (2012). An additional paralarva collected during the project FishJelly with a Bongo net with a 40 cm diameter opening and a mesh size of 300 µm in the autumn of 2014 was also analysed from the NW Mediterranean. These zooplankton samples were fixed in 5% formaldehyde buffered with sodium tetraborate. Ommastrephid paralarvae were distinguished from the other cephalopod paralarvae by the presence of the proboscis. The general morphology of the fixed specimens (chromatophores, size, number of arms, etc.) was examined under the stereomicroscope prior to observation under SEM as described previously.

The specimen from the MAFIA cruise was frozen and measurements were taken after defrosting. All of these paralarvae were identified using the dichotomous key developed in the present study.

Results

Morphological description of the rhynchoteuthion hatchlings from the NE Atlantic.

Morphology of rhynchoteuthion paralarvae is very similar among species: hatchlings usually have only one sucker on both pairs of arms I and II, pair IV is a protuberance without suckers and pair III is totally undeveloped. Morphometric measurements and indices for each species are shown in Table 1. Morphometric comparisons between species were performed based on the indices, rather than on the raw measures. A full description of the chromatophore pattern of each species is provided in Table 2. The rhynchoteuthion species Type in relation to ratio of proboscis sucker size and the description of the proboscis and arm sucker pegs is summarized in Table 3.

Illex coindetii hatchlings

The general morphology of the hatchling (Fig. 1a-d, 3a-c) of this species does not diverge from that described for the congeneric *I. argentinus* (Sakai et al., 1998). The mean VML is 1.41 ± 0.15 mm. On the head, there are 2 ventral chromatophores, one below each eye, and dorsally there are two rows of chromatophores, the first formed by a single chromatophore anterior to the eyes and the second formed by 3 chromatophores at the base of the head. In some individuals, small dark brown pigmented dots appear on the tips of the arms and proboscis (Figs. 1b, d and 3b). Although uncommon, some individuals showed head chromatophores arranged asymmetrically, generally placed on the lateral sides of the head. On the mantle, there are up to 6 rows ventrally, distributed as follows: 4 + 2 + 4 + 3+ 3+ 2; dorsally, there are up to 5 rows: 2 + 3 + 3 + 0 + 1. The 8 suckers are of similar size (35.1 ± 3.9 µm) (Type C rhynchoteuthion, Fig. 2a) and have only one row of pegs (12.9 ± 1.4) (Table 3, Fig. 2c), but additional asymmetrically distributed pegs can be found outside of this row. The arm suckers measure 40.2 ± 2.3 µm in diameter and bear two rows of pegs (Fig. 2b), the internal one with 12.1 ± 1.0 pegs, the external one with 12.2 ± 1.4. A few pegs can appear externally to the external row (Fig. 2b). The skin is smooth and does not have any special sculpture (Fig. 2d). When compared with the other paralarvae described here (Table 1), the FuLI and PWI are larger, which indicates that the funnel is comparatively larger than in the other two species (although the range of this index overlaps with that of *T. eblanae*); and the proboscis is wider, although some overlap exists.

Remarks: Moreno (2008: Fig. 4.18) tentatively identified rhynchoteuthion paralarvae based on the drawings of Salman, Katagan & Benli (2003, see below for more details) and among these, some were identified as *Illex* specimens. Her pictures clearly show a Type C rhynchoteuthion without ocular or intestinal photophores. Thus, these specimens were either *I. coindetii* or *T. eblanae*. However, the identification of these specimens could not be confirmed from the available description and pictures.

Roura (2013) succeeded in molecularly identifying one *I. coindetii* paralarva out of the 15 barcoded from Cape Silleiro (north-western coast of the Iberian Peninsula). However, he did not provide any morphological description of these paralarvae.

Todarodes sagittatus hatchlings

The general morphology of this hatchling (Fig. 1e-h, 3d-f) is similar to the congeneric *T. pacificus* (Watanabe et al., 1996; Puneeta et al., 2015). The mean VML is 1.64 ± 0.12 mm. On the head, there are no ventral chromatophores. Dorsally there are two rows of chromatophores, the first formed by a single chromatophore anterior to the eyes and the second formed by 3 chromatophores at the base of the head. On the mantle, there are up to 4 rows ventrally, distributed as follows: 2 + 6 + 5 + 2; dorsally, there are up to 5 rows, with the following configuration: 3 + 1 + 4 + 0 + 0. The lateral proboscis suckers are larger in size (41.2 ± 8.0 µm) than the medial suckers (35.0 ± 6.7 µm) (Type B rhynchoteuthion, Fig. 2e). The ratio between the size of the sucker diameter of the lateral suckers and the medial suckers is 1.2:1. Two rows of pegs are found (Fig. 2g), the internal row with 18.0 ± 3 and the external with 17.0 ± 3 pegs. There are no differences in the number or arrangement of the sucker pegs between lateral and medial suckers. All pegs belonged to either of these two rows. The skin of this species shows a hexagon-like structure under the stereomicroscope (Fig. 2h). The FuLI (Table 1) is comparatively smaller than in *I. coindetii* and *T. eblanae*, showing a shorter funnel.

Remarks: Salman et al. (2003: Fig. 7) identified 2 rhynchoteuthions from the Aegean Sea as *I. coindetii*. However, the drawing of the proboscis tip clearly shows a type B rhynchoteuthion paralarva. The value of the ratio of sucker sizes is 1.4:1. No photophores were drawn and *H. pelagica* and *O. antillarum* have never been found in Mediterranean waters (Jereb & Roper, 2010), excluding the other Type B paralarva from the NE Atlantic area. Although the ratio of sucker sizes does not fit accurately with the value obtained here for *T. sagittatus* (1.2:1), we considered these two paralarvae as members of this species, rather than *I. coindetii*. Possible sources of this variation could be: a) differences related to the developmental state, since those drawn for Salman et al. (2003) show more than one sucker on each arm and are of a larger size (2.5-3.5 mm ML); b) intraspecific or regional variation; c) differences related to the fixation procedure, since plankton samples usually are not anaesthetized before fixation and some contraction is expected to occur; d) lower levels of accuracy in the measurements from the drawings.

Moreno (2008) described a rhynchoteuthion paralarva with lateral suckers larger than the medial ones in Atlantic Iberian waters. It is not possible to take measurements from the pictures (Moreno, 2008: Fig. 4.22c) due to the orientation of the animal. No evidence of eye photophores is found based on the pictures. However, the chromatophore pattern of both dorsal and ventral views of the head and mantle is visible. The chromatophore pattern of the ventral surface of the mantle is 4 + 4 + 4 + 1 + 1 and for the dorsal surface 3 + 4 + 3 + 2. The dorsal chromatophore pattern of the head is not fully visible, but in the ventral view no chromatophores appear. The chromatophore pattern of this individual is consistent with that described for *T. sagittatus* in this work, especially regarding the absence of ventral chromatophores on the head in the hatchlings of this species, which is of high taxonomic significance.

An 18 mm TL juvenile individual assigned to *T. sagittatus* sampled in Sicily (Central Mediterranean Sea) has been documented (Piatkowski et al., 2015: Fig. 16.4). The absence of chromatophores on the ventral surface of the head is remarkable. Although this observation is based only on one specimen and more observations are necessary, this fact stresses this character as highly diagnostic for this species, possibly throughout its life as a rhynchoteuthion.

The rhynchoteuthion paralarvae of the congeneric species *T. pacificus* differ from *T. sagitattus* in their smaller size (up to 1.4 mm ML, Puneeta et al., 2015: Fig. 9), the chromatophore pattern

(see Discussion) and the proboscis suckers, which are of equal size in *T. pacificus* (Puneeta et al., 2015: Fig. 8). Therefore, this constitutes a Type C rhynchoteuthion.

Todaropsis eblanae hatchlings

This species is the largest rhynchoteuthion hatchling (Table 1) described to date and exhibits more advanced development at the time of hatching than other previously described species (Fig. 1i-l, 2I, 3g-I). In addition to the arm pairs I, II and IV, the pair III arm primordia are present as well (Fig. 2i). While arm pairs I and II possess one sucker, pairs III and IV have no suckers. The mean VML is 2.16 ± 0.11 mm. On the head, there are 2 chromatophores ventrally, one below each eye; dorsally there are three rows of chromatophores, the first formed by a single chromatophore anterior to the eyes, the second formed by two chromatophores at the level of the eyes and the third formed by 3 chromatophores at the base of the head. On the mantle, there are up to 6 rows ventrally, distributed as follows: 7 + 5 + 0 + 0 + 5 + 2; dorsally, there are up to 5 rows: 3 + 0 + 5 + 0 + 2. Between 1 and 4 true lateral chromatophores are present on the mantle (Fig. 3i, Table 2). The 8 proboscis suckers are of similar size (54.3 ± 5.0 µm) (Type C rhynchoteuthion) and have two rows of pegs, the internal one with 18.1 ± 1.0 and the external one with 22.0 ± 2.2 pegs (Fig. 3k), with up to 3 additional pegs asymmetrically distributed outside of the external row. The arm suckers measure 63.0 ± 5.5 µm and bear two rows of pegs (Fig. 2b), the internal one formed by 17.0 ± 0.8 and the external by 20.6 ± 1.5 pegs. Between 0 and 8 pegs arranged externally to the external row can be found asymmetrically scattered. The skin of the species shows a hexagon-like structure under the stereomicroscope (Fig. 2l). DMLI is smaller than in the other two species, which indicates a similar length between DML and VML. Although there is some overlap with the other two species, HWI is smaller, and thus the head is narrower. The AIILI shows a larger pair of arms II than *I. coindetii* and *T. sagittatus*.

Remarks: Roura (2013) sequenced two wild rhynchoteuthion paralarvae which did not produce a species-level match with any previously sequenced ommastrephid. He hypothesized that those collected in the oceanic realm should be assigned to *Todarodes sagitattus* and those from the shelf should be assigned to *Todaropsis eblanae*. The recent work of Gebhardt & Knebelsberger (2015) provided available barcodes for these two species, which could be used to positively identify wild rhynchoteuthions by DNA barcoding (Hebert et al., 2003). A BLAST (Altschul et al., 1990) search shows that the sequence with the GenBank accession number LN614712, uploaded and identified as *T. eblanae* by Roura, does represent an individual of this species.

Ommastrephes bartramii paralarvae (Fig. 3j-k)

The following description is based on Sweeney et al. (1992), Young & Hirota (1990) Sakurai et al. (1995) and Vijai et al. (2015). The hatchling bears the pairs of arms I, II and IV, the latter devoid of suckers. On the head, there is a row of two ventral chromatophores; dorsally, there are two rows formed by 1 and 2 chromatophores, respectively. On the mantle, the ventral surface has up to 3 rows with the following formula: (3-4) + (0-1) + 1; dorsally there are up to 2 rows: (4-5) + (0-1). Later (~3 mm DML), two ventrally centred chromatophores appear on the edge of the mantle. The dorsal pattern becomes scattered-like at size ~4 mm mantle length and ventrally at ~6 mm mantle length. The ratio between the lateral and medial proboscis suckers is 2:1 (Type A rhynchoteuthion). There are two rows of pegs on the proboscis suckers. There are more pegs on the lateral suckers (~20 internal, ~27 external) than on the medial ones (~11 internal, ~14

external). The skin shows a hexagon-like structure under the stereomicroscope (Vijai et al., 2015: Fig 7j-m).

Sthenoteuthis pteropus paralarvae (Fig. 3n)

The following descriptions are based on Sweeney et al. (1992). This species is characterized by the presence of two equally-sized intestinal photophores and another single photophore on the ventral surface of each eye. The chromatophore pattern has not been described for this species. There are no size differences among the proboscis suckers (Type C rhynchoteuthion). The pegs of the proboscis suckers are unknown.

Hyaloteuthis pelagica paralarvae (Fig. 3l-m)

The following descriptions are based on Harman & Young (1985), Sweeney et al. (1992) and Diekmann et al. (2002). This paralarva bears one central intestinal photophore and another on the ventral surface of each eye. According to Diekmann et al. (2002: Table 5), the intestinal photophore is visible in individuals of 1.5 mm ML or larger. The chromatophore pattern is formed by highly scattered units on both the mantle and head. On the head, one chromatophore is located on the ventral surface of each eye and another one is located on the dorsal surface of the eye. On the head, dorsally there are four rows of chromatophores (excluding the ocular chromatophores): 1 + 2 + 1. Individuals smaller than 2 mm of DML lack chromatophores on the ventral surface of the mantle; later a single row of chromatophores on the anterior edge and four chromatophores forming a diamond-shape pattern between the fins appear. Dorsally on the mantle, a single large chromatophore is present on the first third of the mantle surface during most of its life as a rhynchoteuthion. The ratio of the proboscis suckers is between 1.25:1 and 1.5:1 (Type B rhynchoteuthion). There are two rows of pegs on the proboscis suckers. There are more pegs on the lateral suckers (14-16 internal, 18-19 external) than on the medial ones (8-11 internal, 8-15 external).

Ornithoteuthis antillarum paralarvae (Fig. 3o)

The following description is based on Sweeney et al. (1992) and Diekmann et al. (2002). This paralarva has single and round ventral photophores on the ventral surface of each eye and two unequally-sized intestinal photophores: the anterior one appears first (Sweeney et al., 1992), but the posterior one grows larger (Diekmann et al., 2002: Table 5). The chromatophore pattern is not known. The ratio of the proboscis suckers is up to 1.5:1 (Type B rhynchoteuthion). The pegs of the proboscis suckers are not known.

Key for the NE Atlantic rhynchoteuthion paralarvae

The primary characters of this key are the size of the proboscis suckers, the presence/absence of photophores and the arrangement of the proboscis sucker pegs. Although the first two characters are observable under a standard stereomicroscope, the proboscis pegs should be observed by specialized microscopy methods, such as SEM. Since the number and arrangement of the chromatophores are variable during the ontogeny of the rhynchoteuthions, we only use these characters when they are taxonomically significant (key step 3a).

1a. Ratio of sucker sizes of 2:1 (Type A rhynchoteuthion), two rows of pegs in proboscis suckers. More pegs in the lateral proboscis suckers (~20 internal, ~27 external) than in the medial ones (~11 internal, ~14 external). Photophores absent.

Ommastrephes bartramii

1b. Ratio of sucker sizes lower than 2:1 **2**

2a. Ratio of sucker sizes between 1.1:1 and 1.9:1 (Type B rhynchoteuthion) **3**

2b. Ratio of sucker sizes of 1:1 (Type C rhynchoteuthion) **5**

3a. Absence of intestinal or ocular photophores, two rows of pegs in proboscis suckers (12-24 internal, 12-22 external), no differences in the number of pegs between lateral and medial proboscis suckers. No ventral head chromatophores.

Todarodes sagittatus

3b. With ocular and intestinal photophores. **4**

4a. Presence of one central intestinal photophore. More pegs in the lateral proboscis suckers (14-16 internal, 18-19 external) than in the medial ones (8-11 internal, 8-15 external).

Hyaloteuthis pelagica

4b. Presence of two unequal intestinal photophores, the posterior one larger than the first one, proboscis sucker pegs unknown.

Ornithoteuthis antillarum

5a. Presence of two equally-sized intestinal photophores and another single photophore on the ventral surface of each eye, proboscis sucker pegs unknown.

Sthenoteuthis pteropus

5b. Without intestinal or ocular photophores **6**

6a. Only one row of pegs on the proboscis suckers (10-14, 1-12 free ones), skin without a hexagon-like pattern.

Illex coindetii

6b. Two rows of pegs (16-24 internal, 17-27 external plus 0-3 free ones) on the proboscis suckers, presence of the 3rd pair of arms at the time of hatching, skin with a hexagon-like pattern.

Todaropsis eblanae

Test of the dichotomous key using wild rhynchoteuthion paralarvae

Fourteen of the 16 rhynchoteuthions examined were successfully identified with the aid of the key: 9 belonged to *I. coindetii*, 4 to *T. sagittatus* and 1 to *S. pteropus* (Table 4, Fig. 4). Among those not identified to the species level with the key there is a Type C paralarva with 2 rows of dorsal head chromatophores (Fig. 4b), compatible with the pattern of *I. coindetii* and not with *T. eblanae*. Thus, this emphasizes the utility of the chromatophore pattern for the identification of hatchlings when other characters are not available. The second unidentified rhynchoteuthion is a Type C paralarva without photophores. It was not possible to determine whether it was *I. coindetii* or *T. eblanae*. Fifteen of the specimens were obtained in the Mediterranean Sea: this is

the first time that identification of Mediterranean ommastrephid paralarvae from formalin-preserved plankton samples is possible with certainty. In general, the most useful characters for the identification of the paralarvae are: 1) the size of the proboscis suckers, 2) the presence/absence of ocular or intestinal photophores and 3) the proboscis pegs.

Discussion

Previous studies have stressed the difficulties of identifying ommastrephid paralarvae from plankton samples (Collins et al., 2002; Gilly et al., 2006; Moreno, 2008; Moreno et al., 2009; Roura, 2013; Zaragoza et al., 2015). Morphological clusters could sometimes be identified based only on the paralarvae morphology, but it was not possible to confirm the species (e. g. Roper & Lu, 1979; Vecchione et al., 2001; Moreno, 2008). Other times, species have been identified based on the adult characters that could be seen in the paralarvae, such as photophores (e. g. Sweeney et al., 1992). Three different sources of paralarval species confirmation could be used, namely: a) aquarium spawning, b) *in vitro* fertilization and c) molecular methods. The first method is limited by the difficulties in catching, housing and maintaining broodstock and inducing spawning (Durward et al., 1980; Bower & Sakurai, 1996). The last method is constrained by the need for previous molecular data obtained from properly identified adults, which may not exist for some species (Roura, 2013). Thus, the main advantage of using *in vitro* fertilization is that the species identification of the paralarvae produced is ensured. Here, this method was successfully used to describe the paralarvae morphology of three ommastrephid species.

Towards the reliable morphological identification of rhynchoteuthion paralarvae: which are the most useful characters?

The morphological description of *I. coindetii*, *T. sagittatus* and *T. eblanae* revealed new taxonomic characters that permit the identification of rhynchoteuthion paralarvae collected in plankton samples from the NE Atlantic. In the case of *I. coindetii*, when alive, they can be easily identified by the absence of any special skin sculpture (Fig. 2d), a character shared with the congeneric *I. argentinus* (Sakai et al., 1998: Fig. 4). Skin sculpture is present in fresh *T. sagittatus* and *T. eblanae* (Fig. 2h, l, respectively), *T. pacificus* (Watanabe et al., 1996: Fig. 7; Puneeta et al., 2015: Fig. 8), *O. bartramii* (Vijai et al., 2015: Fig 7j-m) and *Dosidicus gigas* (d'Orbigny, 1835: 50 [in 1834–1847]) (D. Staaf, pers. comm.). This skin sculpture is an optical effect created by light that crosses vertical expansions of the basal membrane of the outer epithelium between the mucous cells (F. Á. Fernández-Álvarez, unpubl. observation). Thus, the absence of this skin sculpture in hatchlings seems to be a synapomorphy of the genus *Illex*. When dealing with fixed specimens, the presence of only one row of pegs in the proboscis suckers allows *I. coindetti* to be differentiated from other sympatric rhynchoteuthions described to date.

Todarodes sagittatus has a type B paralarva, a condition that differentiates this species from sympatric ommastrephids, except for *H. pelagica* and *O. antillarum*, which bear ocular and intestinal photophores, with the former bearing a peculiar chromatophore pattern. When we compare *T. sagittatus* hatchlings with the congeneric species *T. pacificus* (Watanabe et al., 1996), the main difference is the absence of ventral head chromatophores in *T. sagittatus*. Based on the chromatophore pattern depicted by Watanabe et al. (1996: Fig. 8), *T. pacificus* bears 5 rows on the ventral surface of the mantle, whereas *T. sagittatus* hatchlings have 3-4 (Table 2). The specimens of *T. pacificus* depicted by Puneeta et al. (2015) are Type C rhynchoteuthions,

however more accurate information on the structure of the proboscis suckers, such as the arrangement of pegs of the suckers, is lacking for comparison against *T. sagittatus*.

Todaropsis eblanae is the largest rhynchoteuthion hatchling described so far and the presence of the third arm buds at hatching is a diagnostic character that differs from other described rhynchoteuthion hatchlings. It can be easily differentiated from *S. pteropus* (also Type C rhynchoteuthion) because it has no photophores. It can also be differentiated from *I. coindetii* because *T. eblanae* has two rows of pegs in the proboscis suckers and a hexagon-like skin sculpture. The morphological descriptions provided here for *I. coindetii*, *T. sagittatus* and *T. eblanae* paralarvae were based on hatchlings and some characters are known to change during their development (see below), such as morphometrics (Table 1) and the chromatophore pattern (Table 2). However, the structure of the eight proboscis suckers (Table 3) is unlikely to change during the rhynchoteuthion phase (see below).

Ommastrephes bartramii is unlikely to be confused with other rhynchoteuthions present in the NE Atlantic, as it is the only Type A rhynchoteuthion in these waters. However, in other areas of its known distribution, this species overlaps with other species with this type of paralarva, such as one of the species of the genus *Ornithoteuthis* Okada, 1927 (Wakabayashi et al., 2002): *Ornithoteuthis volatilis* (Sasaki, 1915). This species is sympatric with *O. bartramii* in both the Pacific and Indian Oceans, but its rhynchoteuthion has fewer pegs on the lateral proboscis suckers (Wakabayashi et al., 2002: Table 6). Moreover, *Ornithoteuthis* rhynchoteuthions have two intestinal photophores (Sweeney et al., 1992; Diekmann et al., 2002: Table 5). It is not clear if *Nototodarus* Pfeffer, 1912 species are Type B or A rhynchoteuthions or both (Sweeney et al., 1992). Since these species also lack photophores, they are the only species that may be misidentified as *O. bartramii* in areas where their distribution overlaps. More research is needed to clarify the morphology of *Nototodarus* paralarvae.

The presence of two intestinal photophores in *S. pteropus* can easily differentiate this species from *H. pelagica* (which has a single round intestinal photophore) in the NE Atlantic, in addition to the proboscis suckers (Type C in the first species, Type B in the second one). *Ornithoteuthis antillarum* also has two intestinal photophores, however the presence of large lateral suckers and the unequal size of the intestinal photophores in *O. antillarum* distinguishes the two species.

The presence of a single intestinal photophore differentiates *H. pelagica* from the other rhynchoteuthions from the NE Atlantic. The proboscis sucker pegs of *H. pelagica* were studied by Harman & Young (1985), showing a pattern with ~14 internal, ~17 external pegs in the lateral suckers and ~9 internal, ~10 external in the medial ones. However, another type B species with a single intestinal photophore, *Eucleoteuthis luminosa* (Sasaki, 1915), is sympatric throughout the distribution area of *H. pelagica* with the exception of the entire North Atlantic. For both species, the proboscis sucker pegs have been described (Harman & Young, 1985 for *H. pelagica* and Wakabayashi et al., 2002 and Granados-Amores et al., 2013 for *E. luminosa*), and the number of pegs in the proboscis suckers seems to be higher than in *H. pelagica*, although some overlap exists (Wakabayashi et al., 2002: Table 4). Wakabayashi et al. (2006) and Granados-Amores et al. (2013) molecularly identified paralarvae of *E. luminosa*, validating its description.

Ornithoteuthis antillarum can be easily differentiated from other Type B rhynchoteuthions by its two unequally-sized photophores. This character also differentiates this species from *E.*

luminosa in the S Atlantic. The congeneric *O. volatilis* is a Type A rhynchoteuthion (Wakabayashi et al., 2002), while *O. antillarum* is a Type B rhynchoteuthion (Diekmann et al, 2002).

Based on the information presented above, it is possible to evaluate the reliability of identifications of rhynchoteuthions based on each taxonomic character. Although the chromatophore pattern led to the correct identification of a *T. sagittatus* specimen from the literature and an *I. coindetii* specimen from our wild collected paralarvae (see above and Table 4, Fig. 4b-c), it should be noted that this pattern changes during the ontogeny (e.g. Young & Hirota, 1990). The same occurs with morphometrics: the shape of the body of rhynchoteuthion paralarvae changes with the size of the animal (e.g. Young & Hirota, 1990, Vidal, 1994 or Gilly et al., 2006) and the different morphometric indices change during ontogeny (Ramos-Castillejos et al., 2010). Although differences between the number of pegs on arm suckers do exist between species (Table 3), comparisons are only possible between paralarvae of similar sizes (in the case of the three rhynchoteuthion species described here, hatchlings and the immediately following stages). Moreover, while the paralarva grows, more suckers are added to the arms, making it difficult to identify each single sucker. As can be seen in Ramos-Castillejos et al. (2010) and Wakabayashi et al. (2002), the number of pegs per row on arm suckers increases while the paralarva grows. Thus, we do not recommend relying only on chromatophore pattern, morphometrics and arm sucker pegs, without the support of others characters for identification purposes. A combination of both proboscis suckers and photophores seems to be the most reliable combination. Photophores are easy to find under the stereomicroscope, both in fresh and fixed specimens. However, no member of the subfamilies Illicinae Posselt, 1891 or Todarodinae Adam, 1960 is known to possess photophores. Together these subfamilies represent 64% of the species biodiversity among the Ommastrephidae. Moreover, this character should be considered with caution since it is not known when photophores appear in some species (Sweeney et al., 1992; Diekmann et al., 2002) and at least in *D. gigas* some variation for photophore appearance during ontogenetic development is suspected (Gilly et al., 2006 found paralarvae of this species with the typical photophores present in the juvenile). Again, by using a binocular microscope it is easy to differentiate between rhynchoteuthion Types A, B and C. When species of the same Type coexist (*I. coindetii* and *T. eblanae* in NE Atlantic), the best approach is to study the proboscis pegs by SEM (Table 4, Fig. 4a). While an individual is a rhynchoteuthion, they have the same 8 proboscis suckers until the proboscis splits and the animal becomes a juvenile (Shea, 2005; Wakabayashi et al., 2002). As Ramos-Castillejos et al. (2010: Fig. 9) have shown for *D. gigas*, the number of internal and external pegs in the 8 proboscis suckers remains the same throughout the rhynchoteuthion stage.

The search for the hatchling stage in ommastrephids

An unresolved discussion remains regarding which of the embryological stages described for ommastrephid squids represents the actual hatchling. This question was raised by Watanabe et al. (1996), who observed a two-stage delay between hatching from aquaria-spawning eggs and those from *in vitro* fertilization in *T. pacificus*. They hypothesize that the hatching stage should be addressed between stages XXV and XXVII, because Hoyle´s organ was visible during these stages. A similar observation was reported by Staaf et al. (2008) for *D. gigas*. Recently, Puneeta et al. (2015) observed hatchlings of stage XXXI from aquarium-spawned *T. pacificus*. In short, although several experiments with eggs obtained by *in vitro* fertilization and by aquaria-spawning in ommastrephids have been performed, the question is unresolved.

In naturally-hatched individuals the development of the characteristics that allow them to swim and avoid predators is expected. However, individuals at stages XXIX or younger never have a fully developed ink sac, fins or statoliths. Thus, correct swimming is not possible at this time and these individuals can only perform horizontal movements on the bottom of the Petri dish, probably by using cilia on the skin (R. Villanueva, unpubl. observation). Additionally, in the case of *T. pacificus* (Watanabe et al., 1996), *T. sagittatus* and *T. eblanae*, fins are not fully developed until stage XXXII. In the present study, the criteria to select a stage as hatchling was a paralarva capable of swimming, with a fully developed ink sac, statoliths and fins as wide as the head. This definition corresponds to stages beyond XXX (*sensu* Sakai et al., 1998) for *Illex* and XXXII (*sensu* Watanabe et al., 1996) for *Todarodes* and *Todaropsis*. Taking into account these criteria, any stage below XXXII should not be addressed as the hatchling for *O. bartramii*, based on the description by Vijai et al. (2015). In addition to these arguments, individuals less developed than those considered here are never reported from plankton samples (for instance, a paralarva without fins). The presence of these prematurely hatched individuals, in our opinion, does not indicate the natural hatchling stage and is a probable consequence of suboptimal artificial conditions in the laboratory (Villanueva et al., 2011). Better culture conditions would likely produce hatchlings that are morphologically more similar to those produced in the wild as the results reported by Puneeta et al. (2015) suggest.

Conclusions

Comprehensive knowledge on the life cycle of ommastrephid squids is hindered by the fact that many aspects of the first stages of their life cycle remain a mystery, especially regarding the paralarvae. For instance, we still do not know the main diet of early rhynchoteuthions as their stomachs are usually empty or contain unrecognized food (e.g. Uchikawa et al., 2009; Camarillo-Coop et al., 2013). Vidal & Haimovici, (1998) have found microorganisms (ciliates, flagellates and bacteria) with mucus inside the digestive tract of early rhynchoteuthions and copepod appendages on the digestive tracts of paralarvae > 3.7 mm ML; together these observations indicate that ommastrephid paralarvae certainly adopt different feeding strategies as they grow (Uchikawa et al., 2009; Shea, 2005). This lack of knowledge inevitably leads to a total failure when any culture experiment is attempted (e. g. Yatsu, Tafur & Maravi, 1999; Staaf et al., 2008). Thus, the little knowledge available on paralarvae beyond yolk consumption proceeds from paralarvae collected in the wild, including the morphology of post-hatchlings (e. g. Young & Hirota, 1990), the bathymetric layers suitable for their development (e. g. Roper & Lu, 1979), their distribution (e.g. Staaf et al., 2013) and the tentative length of the paralarval period (e. g. Uchikawa et al., 2009). Clearly, if our knowledge in all these matters relies on wild collected paralarvae, a well-established taxonomic knowledge of each species for reliable identification is necessary. Here, we fill a gap in the knowledge of NE Atlantic rhynchoteuthions by describing the morphology of three of the seven species and used this new knowledge in conjunction with the literature to develop the first dichotomous key covering all the ommastrephid squid paralarvae present in a wide area. Moreover, this methodology was applied to identify 16 plankton sampled ommastrephid paralarvae and, for the first time, data on properly identified paralarvae was provided for the Mediterranean Sea. This key will permit the identification of rhynchoteuthions from plankton samples collected in the NE Atlantic, thus providing a useful tool for future studies on the planktonic life and population dynamics of ommastrephid squids.

Acknowledgements

We greatly appreciate the help with squid collection of the crew of the following trawlers: *Pilar Rus*, *La Seu*, *Avi Pau*, *Pilar Peña*, *Montserrat*, *Silvia i Ben* (Vilanova i la Geltrú) and *Maireta IV* (Barcelona); and Elisabeth Cuesta-Torralvo for her support during collecting samples. Thanks to José Manuel Fortuño for his dedication and kindness during the SEM sessions. Thanks are due to Ana Sabatés and Vanesa Raya, for providing the wild rhynchoteuthion paralarvae collected during the research project CACO (REN2002-01339/MAR) and Laura Recasens and Pilar Olivar for those collected on the LLUÇ3 cruise. María Pascual kindly provided us with the wild paralarva from the project FishJelly. The *Sthenoteuthis pteropus* specimen was collected on board the RV Hesperides during the research project MAFIA (CTM2012-39587-C04-03), funded by the Spanish Ministry of Economy and Competitiveness (MINECO). Thanks to Dr. Louise Allcock and three anonymous reviewers for their comments. FAFA was supported by a predoctoral fellowship of the MINECO (BES-2013-063551). EAGV was supported by the Brazilian National Research Council-CNPq (Grants no. 207680/2014-0, 250017/2013-0). This study was funded by the research projects CALOCEAN-1 (AGL2009-11546) and CALOCEAN-2 (AGL2012-39077) from the MINECO.

References

Adam W. 1957. Notes sur les Céphalopodes. XXIII – Quelques espèces des Antilles. *Bulletin de l'Institut Royal des Sciences Naturelles de Belgique* 33: 1-10.

Adam W. 1960. Notes sur les Cephalopodes XXIV: Contribution a la connaissance de l'hectocotyle chez les Ommastrephidae. *Bulletin de l'Institut Royal des Sciences Naturelles de Belgique* 36: 1-10.

Adam W. 1962. Céphalopodes de l'Archipel du Cap-Vert, de l'Angola et du Mozambique. *Memorias da Junta de Investigacoes do Ultramar (2ª Série)* 33: 9-64.

Altschul SF, Gish W, Miller W, Myers EW, Lipman DJ. 1990. Basic local alignment search tool. *Journal of Molecular Biology* 215: 403-410.

Arkhipkin AI, Rodhouse PGK, Pierce GJ, Sauer W, Sakai M, Allcock L, Arguelles J, Bower JR, Castillo G, Ceriola L, Chen C-S, Chen X, Diaz-Santana M, Downey N, González AF, Granados Amores J, Green CP, Guerra A, Hendrickson LC, Ibáñez C, Ito K, Jereb P, Kato Y, Katugin ON, Kawano M, Kidokoro H, Kulik VV, Laptikhovsky VV, Lipinski MR, Liu B, Mariátegui L, Marin W, Medina A, Miki K, Miyahara K, Moltschaniwskyj N, Moustahfid H, Nabhitabhata J, Nanjo N, Nigmatullin CM, Ohtani T, Pecl G, Perez JAA, Piatkowski U, Saikliang P, Salinas-Zavala CA, Steer M, Tian Y, Ueta Y, Vijai D, Wakabayashi T, Yamaguchi T, Yamashiro C, Yamashita N, Zeidberg LD. 2015. World Squid Fisheries. *Reviews in Fisheries Science & Aquaculture* 23: 92-252.

Ball R. 1841. On a species of *Loligo*, found on the shore of Dublin Bay. *Proceedings of the Royal Irish Academy* 1: 362-364.

Berry SS. 1912. A catalogue of Japanese Cephalopoda. *Proceedings of the Academy of Natural Sciences of Philadelphia* 64: 380-444.

Boletzky SV, Rowe L, Aroles L. 1973. Spawning and development of the eggs, in the laboratory, of *Illex coindetii* (Mollusca: Cephalopoda). *Veliger* 15: 257-258.

Bosc LAG. 1802. *Histoire naturelle des vers contenant leur descriptionet leurs moeurs; avec figures dessinees d'apres nature*. Paris: Déterville.

Bower JR, Sakurai Y. 1996. Laboratory observations on *Todarodes pacificus* (Cephalopoda: Ommastrephidae) egg masses. *American Malacological Bulletin* 13: 65-71.

Boyle PR, Rodhouse PG. 2005. *Cephalopods. Ecology and Fisheries*. Oxford: Blackwell Science Ltd.

Brasseur P, Beckers JM, Brankart JM, Schoenauen R. 1996. Seasonal temperature and salinity fields in the Mediterranean Sea: Climatological analyses of a historical data set. *Deep-Sea Research I* 43: 159-192.

Brunetti NE. 1990. An scale for identification of stages of sexual maturity in the Argentine squid (*Illex argentinus*). *Frente Maritimo* 7: 45-51.

Camarillo-Coop S, Salinas-Zavala CA, Lavaniegos BE, Markaida U. 2013. Food in early life stages of *Dosidicus gigas* (Cephalopoda: Ommastrephidae) from the Gulf of California, Mexico. *Journal of the Marine Biological Association of the United Kingdom* 93: 1903-1910.

Carlini DB, Kunkle LK, Vecchione M. 2006. A molecular systematic evaluation of the squid genus *Illex* (Cephalopoda: Ommastrephidae) in the North Atlantic Ocean and Mediterranean Sea. *Molecular Phylogenetics and Evolution* 41: 496-502.

Castellanos ZJA. 1960. Una nueva especie de calamar Argentino, *Ommastrephes argentinus* sp. nov. (Mollusca, Cephalopoda). *Neotropica* 6: 55-58.

Coll M, Navarro J, Olson RJ, Christensen V. 2013. Assessing the trophic position and ecological role of squids in marine ecosystems by means of food-web models. *Deep-Sea Research II* 95: 21-36.

Collins MA, Yau C, Boyle PR, Friese D, Piatkowski U. 2002. Distribution of cephalopods from plankton surveys around the British Isles. *Bulletin of Marine Science* 71: 239-254.

Diekmann R, Piatkowsky U, Schneider M. 2002. Early life and juvenile cephalopods around seamounts of the subtropical eastern North Atlantic: Illustrations and a key for their identification. *Berichte aus dem Institut für Meereskunde an der Christian-Aabrechts-Universität Kiel* 326: 1-42.

D'Orbigny A. 1835 (1834-1847). Mollusques. *Voyage dans l'Amerique Meridionale* 5: 1-758.

Durward RD, Vessey E, O'Dor RK, Amaratunga T. 1980. Reproduction in the squid, *Illex illecebrosus*: first observation in captivity and implications for the life cycle. *International Commision for the Nortwest Atlantic Fisheries Selected Papers* 6: 7-13.

Gebhardt K, Knebelsberger T. 2015. Identification of cephalopod species from the North and Baltic Seas using morphology, COI and 18S rDNA sequences. *Helgoland Marine Research* 69: 259-271.

Gilly WF, Elliger CA, Salinas CA, Camarilla-Coop S, Bazzino G, Beman M. 2006. Spawning by jumbo squid *Dosidicus gigas* in San Pedro Mártir Basin, Gulf of California, Mexico. *Marine Ecology Progress Series* 313: 125-133.

Granados-Amores J, Ramos JE, Salinas-Zavala CA, Camarillo-Coop S. 2013. *Eucleoteuthis luminosa* (cephalopoda: ommastrephidae) off the west coast of the Baja California Peninsula, Mexico. *Journal of Shellfish Research* 32: 341-346.

Harman RF, Young RE. 1985. The larvae of ommastrephid squids (Cephalopoda, Teuthoidea) from Hawaiian waters. *Vie Milieu* 35: 211-222.

Hebert PD, Cywinska A, Ball SL, deWaard JR. 2003. Biological identifications through DNA barcodes. *Proceedings of the Royal Society B: Biological Sciences* 270: 313-321.

Jereb P, Roper CFE. 2010. *Cephalopods of the world. An annotated and illustrated catalogue of cephalopod species known to date. Vol 2. Myopsid and Oegopsid Squids*. Rome: FAO.

Lamarck JB. 1798. Extrait d'un mémoire sur le genre de la Séche, du Calmar et Poulpe, vulgairement nommés, Polypes de Mer. *Bulletin des Sciences, par la Société Philomatique de Paris* 2: 129-131.

Lesson RP. 1830-1831. *Voyage autour du monde: exécuté par ordre du Roi, sur la corvette de Sa Majesté, la Coquille, pendant les années 1822, 1823, 1824, et 1825*. Paris: A. Bertrand.

Lesueur CA. 1821. Descriptions of several new species of cuttlefish. *Journal of the Academy of Natural Sciences of Philadelphia* 2: 86-101.

Logan JM, Toppin R, Smith S, Galuardi B, Porter J, Lutcavage ME. 2013. Contribution of cephalopod prey to the diet of large pelagic fish predators in the central North Atlantic Ocean. *Deep-Sea Research II* 95: 74-82.

Meillat M. 2012. Essais du chalut mésopélagos pour le programme MYCTO 3D-MAP de l'IRD, à bord du Marion Dufresne. Du 10 au 21 Août 2012. Rapport de mission Marion Dufresne. Unpublished report, Ifremer.

Moreno A. 2008. Geographic variation in cephalopod life history traits. Unpublished "Dissertação apresentada para accesso à categoria de Investigador Auxiliar" Thesis, Unidade de Recursos Marinhos e Sustentabilidade L-IPIMAR.

Moreno A, Santos A, Piatkowski U, Santos AMP, Cabral H. 2009. Distribution of cephalopod paralarvae in relation to the regional oceanography of the western Iberia. *Journal of Plankton Research* 31: 73-91.

Nesis K. 1979. Squid larvae of the family Ommastrephidae (Cephalopoda). *Zoologicheskii Zhurnal* 58: 17-30.

O'Dor RK, Balch N, Foy EA, Hirtle RWM, Johnston DA, Amaratunga T. 1982. Embryonic development of the squid, *Illex illecebrosus*, and effect of temperature on development rates. *Journal of the Northwest Atlantic Fisheries Scien*ce 3: 41-45.

Okada YK. 1927. Contribution à l'etude des céphalopodes lumineaux (notes préliminaires). IV. *Ommastrephes volatilis* Sasaki est une forme lumineaux; établissement d'un nouveau genre: *Ornithoteuthis*. *Bulletin de l'Institut Océanographique de Monaco* 494: 13-16.

Palomera I, Olivar MP, Morales-Nin B. 2005. Larval development and growth of the European hake in North Western Mediterranean. *Scientia Marina* 69: 251-258.

Pfeffer G. 1912. Die Cephalopoden der Plankton-Expedition. Zugleich eine monographische übersicht der Oegopsiden Cephalopoden. *Ergebnisse der Plankton-Expedition der Humboldt-stiftung* 2: 1-815.

Piatkowski U, Zumholz K, Lefkaditou E, Oesterwind D, Jereb P, Pierce GJ, Allcock L. 2015. *Todarodes sagittatus*. European flying squid. Cephalopod biology and fisheries in Europe: II. Species Accounts. *ICES Cooperative Research Report* 235: 193-205.

Posselt HI. 1891. *Todarodes sagittatus* (Lmk.) Stp., En anatomisk studie med Bemaerkinger om Slaegtskabsforholdet mellem Ommatostrephfamiliens Genera. *Videnskabelige Meddelelser fra den Naturhistoriske Forening I Kjobenhavn* 1890: 301-359.

Puneeta P, Vijai D, Yoo H-K, Matsui H, Sakurai Y. 2015. Observations on the spawning behavior, egg masses and paralarval development of the ommastrephid squid *Todarodes pacificus* in a laboratory mesocosm. *Journal of Experimental Biology* 218: 3825-3835.

Ramos-Castillejos JE, Salinas-Zavala CA, Camarillo-Coop S, Enríquez-Paredes LM. 2010. Paralarvae of the jumbo squid, *Dosidicus gigas*. *Invertebrate Biology* 129: 172-183.

Roper CFE, Lu CC. 1979. Rhynchoteuthion larvae of ommastrephid squids of the western North Atlantic, with the first description of larvae and juveniles of *Illex illecebrosus*. *Proceedings of the Biological Society of Washington* 91: 1039-1059.

Roper CFE, Lu CC, Mangold K. 1969. A new species of *Illex* from the Western Atlantic and distributional aspects of other *Illex* species Cephalopoda: Oegopsida). *Proceedings of Biological Society of Washington* 82: 295-322.

Roper CFE, Voss GL. 1983. Guidelines for taxonomic descriptions of cephalopod species. In: Roper CFE, Lu CC, Hochberg FG, eds. Proceedings of the workshop on the biology and resource potential of cephalopods. *Memoirs of National Museum Victoria, Melbourne, Australia* 44: 49-63.

Roura A. 2013. Ecology of planktonic cephalopod paralarvae in coastal upwelling systems. Unpublished D. Phil. Thesis, Vigo University.

Sabatés A, Salat J, Raya V, Emelianov M, Segura-Noguera M. 2009. Spawning environmental conditions of *Sardinella aurita* at the northern limit of its distribution range, the western Mediterranean. *Marine Ecology Progress Series* 385: 227-236.

Sakai M, Brunetti NE, Elena B, Sakurai Y. 1998. Embryonic development and hatchlings of *Illex argentinus* derived from artificial fertilization. *South African Journal of Marine Science* 20: 255-265.

Sakurai Y, Young RE, Hirota J, Mangold K, Vecchione M, Clarke MR, Bower J. 1995. Artificial fertilization and development through hatching in the oceanic squids *Ommastrephes bartramii* and *Sthenoteuthis oualaniensis* (Cephalopoda: Ommastrephidae). *Veliger* 38: 185-191.

Salman A, Katagan T, Benli HA. 2003. Vertical distribution and abundance of juvenile cephalopods in Aegean Sea. *Scientia Marina* 67: 167-176.

Sasaki M. 1915. On three interesting new oegopsids from the Bay of Sagami. *Journal of the College of Agriculture, Tohoku Imperial University, Sapporo* 6: 131-150.

Shea EK. 2005. Ontogeny of the fused tentacles in three species of ommastrephid squids (Cephalopoda, Ommastrephidae). *Invertebrate Biology* 124: 25-38.

Staaf DJ, Camarillo-Coop S, Haddock SHD, Nyack AC, Payne J, Salinas-Zavala CA, Seibel BA, Trueblood L, Widmer C, Gilly WF. 2008. Natural egg mass deposition by the Humboldt squid (*Dosidicus gigas*) in the Gulf of California and characteristics of hatchlings and paralarvae. *Journal of the Marine Biological Association of the United Kingdom* 88: 759-770.

Staaf DJ, Redfern JV, Gilly WF, Watson W, Balance LT. 2013. Distribution of ommastrephid paralarvae in the eastern tropical Pacific. *Fishery Bulletin* 111: 78-89.

Steenstrup J. 1855. Kjaeber af en kolossal Blaeksprutte. *Oversigt over det Kongelige Danske Videnskabernes Selskabs Forhandlinger* 1855: 199-200.

Steenstrup J. 1880. De Ommatostrephagtige Blaeksprutter indbyrdes Forhold. *Oversigt over det Kongelige Danske Videnskabernes Selskabs Forhandlinger* 1880: 73-110.

Sweeney MJ, Roper CFE, Mangold KM, Clarke MR, Boletzky SV. 1992. *"Larval" and juvenile cephalopods: A manual for their identification*. Washington DC: Smithsonian Institution Press.

Uchikawa K, Sakai M, Wakabayashi T, Ichii T. 2009. The relationship between paralarval feeding and morphological changes in the proboscis and beaks of the neon flying squid *Ommastrephes bartramii*. *Fisheries Science* 75: 317-323.

Vecchione M, Roper CFE, Sweeney MJ, Lu CC. 2001. Distribution of paralarval cephalopods in the western North Atlantic with observations on paralarval development. *NOAA Technical Report NMFS* 152: 1-54.

Verany JB. 1839. Memoire sur six nouvelles espèces de Céphalopodes trouves dans la Mediterranee a Nice. *Memorie della Reale Accademia delle Scienze di Torino, (series 2)* 1: 91-98.

Vidal EAG. 1994. Relative growth of paralarvae and juveniles of *Illex argentinus* (Castellanos, 1960) in southern Brazil. *Antarctic Science* 6: 275-282.

Vidal EAG, Haimovici M. 1998. Feeding and the possible role of the proboscis and mucus cover in the ingestion of microorganisms by rhynchoteuthion paralarvae (Cephalopod: Ommastrephidae). *Bulletin of Marine Science* 63: 305-316.

Vijai D, Sakai M, Sakurai Y. 2015. Embryonic and paralarval development following artificial fertilization in the neon flying squid *Ommastrephes bartramii*. *Zoomorphology* 134: 417-430.

Villanueva R, Quintana D, Petroni G, Bozzano A. 2011. Factors influencing the embryonic development and hatchling size of the oceanic squid *Illex coindetii* following *in vitro* fertilization. *Journal of Experimental Marine Biology and Ecology* 407: 54-62.

Villanueva R, Staaf DJ, Argüelles J, Bozzano A, Camarillo-Coop S, Nigmatullin CM, Petroni G, Quintana D, Sakai M, Sakurai Y, Salinas-Zavala CA, De Silva-Dávila R, Tafur R,

Yamashiro C, Vidal EAG. 2012. A laboratory guide to *in vitro* fertilization of oceanic squids. *Aquaculture* 342–343: 125-133.

Wakabayashi T, Saito K, Tsuchiya K, Segawa S. 2002. Descriptions of *Eucloteuthis luminosa* (Sasaki, 1915) and *Ornithoteuthis volatilis* (Sasaki, 1915) paralarvae in the northwestern Pacific. *Venus* 60: 237-260.

Wakabayashi T, Suzuki N, Sakai M, Ichii T, Chow S. 2006. Identification of ommastrephid squid paralarvae collected in northern Hawaiian waters and phylogenetic implications for the family Ommastrephidae using mtDNA analysis. *Fisheries Science* 72: 494-502.

Watanabe K, Sakurai Y, Segawa S, Okutani T. 1996. Development of the ommastrephid squid *Todarodes pacificus*, from fertilized egg to rhynchoteuthion paralarva. *American Malacological Bulletin* 13: 73-88.

Yatsu A, Tafur R, Maravi C. 1999. Embryos and rhynchoteuthion paralarvae of the jumbo flying squid *Dosidicus gigas* (Cephalopoda) obtained through artificial fertilization from Peruvian waters. *Fisheries Science* 65: 904-908.

Young RE, Hirota J. 1990. Description of *Ommastrephes bartramii* (Cephalopoda: Ommastrephidae) paralarvae with evidence for spawing in Hawaiian waters. *Pacific Science* 44: 71-80.

Zaragoza N, Quetglas A, Hidalgo M, Álvarez-Berastegui D, Balbín R, Alemany F. 2015. Effects of contrasting oceanographic conditions on the spatiotemporal distribution of Mediterranean cephalopod paralarvae. *Hydrobiologia* 749: 1-14.

Figure captions

Figure 1. (a-d) *Illex coindetii*. a) Ventral view, aged 354 h and incubated at 17 ºC. b) Dorsal view, aged 427 h and incubated at 17 ºC. c) Lateral view, aged 262 h and incubated at 21 ºC. d) Ventral view of an individual with expanded chromatophores, aged 236 h and incubated at 17 ºC. (e-h) *Todarodes sagittatus*. e) Ventral view, aged 364 h and incubated at 15 ºC. f) Dorsal view, aged 358 h and incubated at 17 ºC. g) Lateral view, aged 360 h and incubated at 17 ºC. h) Ventral view of an individual with expanded chromatophores, aged 336 h and incubated at 17 ºC. (i-l) *Todaropsis eblanae*. i) Ventral view, aged 475 h and incubated at 17 ºC. j) Dorsal view, aged 500 h and incubated at 15 ºC. k) Lateral view, aged 498 h and incubated at 15 ºC. l) Ventral view of an individual with expanded chromatophores, aged 649 h and incubated at 15 ºC. a-c, e-g, i-k, specimens anaesthetized with ethanol, which potentially causes chromatophore contraction. d, h, l, individuals without anaesthesia. Scale bars: 1 mm.

Figure 2. (a-d) *Illex coindetii*. a) SEM image of the ventral view of the head, aged 270 h and incubated at 17 ºC. b) SEM image of the arm I sucker, aged 270 h and incubated at 17 ºC. c) SEM image of a proboscis sucker, aged 454 h and incubated at 17 ºC. d) Detail of the ventral skin of an anaesthetized specimen, aged 329 h and incubated at 21 ºC. (e-h) *Todarodes sagittatus*. e) SEM image of proboscis tip, showing the differences between the lateral and medial suckers, aged 361 h and incubated at 15 ºC. f) SEM image of the left arm I sucker, aged

361 h and incubated at 15 ºC. g) SEM image of a proboscis sucker, aged 361 h and incubated at 15 ºC. h) Detail of the ventral skin of an anaesthetized specimen, aged 383 h and incubated at 15 ºC. (i-l) *Todaropsis eblanae*. i) SEM image of the ventrolateral view of the head of a paralarva, aged 477 h and incubated at 15 ºC, the III and IV pairs of arm stumps are visible. j) SEM image of the sucker of the left arm I, aged 475 h and incubated at 15 ºC. k) SEM image of a proboscis sucker, aged 477 h and incubated at 15 ºC. l) Detail of the ventral skin of an anaesthetized specimen, aged 498 h and incubated at 15 ºC. Scale bars: a, e, i, 100 µm; b, c, f, g, k, 20 µm; j, 50 µm; d, h, l, 0.5 mm.

Figure 3. Schematic drawing of the chromatophore and photophore pattern of the seven North-eastern Atlantic rhynchoteuthions. (a-c) *Illex coindetii*. a) Ventral view. b) Dorsal view. c) Lateral view. (d-f) *Todarodes sagittatus*. d) Ventral view. e) Dorsal view. f) Lateral view. (g-i) *Todaropsis eblanae*. g) Ventral view. h) Dorsal view. i) Lateral view. (j-k) *Ommastrephes bartramii*. j) Ventral view. k) Dorsal view. (l-m) *Hyaloteuthis pelagica*. l) Ventral view. m) Dorsal view. n) *Sthenoteuthis pteropus*, ventral view. o) *Ornithoteuthis antillarum*, ventral view. Grey chromatophores of a-f depict those seen in both dorsal and ventral views. Concentric black and white circles on l-n depict ocular and intestinal photophores. Chromatophore pattern of a-f is based on the mode of the chromatophore pattern (see table 2); j-k based on Sweeney et al. (1992), Young & Hirota, (1990), Sakurai et al. (1995) and Vijai et al. (2015). Photophore and chromatophore pattern of l-m based on Harman & Young (1985) and Sweeney et al. (1992). Photophore pattern of n based on Sweeney et al. (1992), of o based on Sweeney et al (1992) and Diekmann et al. (2002). The chromatophore pattern of *S. pteropus* (n) and *O. antillarum* (o) are not known.

Figure 4. Main taxonomic characters used to identify wild-collected rhynchoteuthions by the dichotomous key provided here. (a-c) *lllex coindetii*. a) 2.4 mm DML. SEM image of the proboscis suckers, showing a single row of pegs. b-c) 1.03 mm DML. b) Dorsal view of the head showing the chromatophore pattern 1 + 3. c) Ventral view of the head showing one row of two chromatophores. (d) *Todarodes sagittatus*, 2.20 mm DML. SEM image of the proboscis suckers showing lateral suckers larger than the medial sucker. (e-g) *Sthenoteuthis pteropus*, 7.71 mm DML. e) Dorsal view of the specimen. f) Ventral view of the head showing the ocular photophores. g) Ventral view of the specimen with the mantle opened to show the two equally-sized intestinal photophores. Scale bars: a, d: 0.1 mm; b-c: 0.5 mm; e-g: 1 mm.

Tables

Table 1. Morphometric parameters measured (mm) and morphometric parameter ratios in relation to the VML (%). Abbreviations: VML: ventral mantle length, DML: dorsal mantle length, TL: total length, TL w P: total length without the proboscis, HL: head length, HW: head width, ED: eye diameter, FuL: funnel length, PW: proboscis width at the base, AIIL: Arm II length, DMLI: dorsal mantle length index, TLI: total length index, TL w PI: total length without the proboscis index, HLI: head length index, HWI: head width index, EDI: eye diameter index, FuLI: funnel length index, PWI: proboscis width at the base index, AIILI: Arm II Length Index.

Species		VML	DML	TL	TL w P	HL	HW	ED	FuL	PW	AIIL	n
Measures												
Illex coindetii	**Average**	1.41	1.52	2.45	2.24	0.52	0.70	0.22	0.73	0.16	0.18	52
	SD	0.15	0.10	0.21	0.20	0.06	0.06	0.03	0.07	0.02	0.06	
	Range	1.09-1.82	1.40-1.71	1.93-2.93	1.65-2.65	0.39-0.67	0.59-0.87	0.16-0.28	0.55-0.91	0.13-0.19	0.10-0.30	
Todarodes sagittatus	**Average**	1.64	1.80	2.63	2.44	0.61	0.79	0.24	0.47	0.16	0.20	29
	SD	0.12	0.14	0.20	0.19	0.08	0.07	0.03	0.04	0.01	0.04	
	Range	1.25-1.81	1.44-1.96	2.03-2.95	1.90-2.73	0.44-0.75	0.64-0.92	0.16-0.30	0.39-0.55	0.14-0.18	0.11-0.26	
Todaropsis eblanae	**Average**	2.16	2.19	3.60	3.26	0.83	1.00	0.34	0.98	0.21	0.41	36
	SD	0.11	0.14	0.24	0.17	0.05	0.06	0.03	0.10	0.01	0.05	
	Range	1.93-2.43	1.92-2.48	3.03-4.12	2.89-3.55	0.71-0.92	0.89-1.10	0.28-0.41	0.74-1.15	0.19-0.25	0.32-0.52	
Ratios			**DMLI**	**TLI**	**TL w PI**	**HLI**	**HWI**	**EDI**	**FuLI**	**PWI**	**AIILI**	
Illex coindetii	**Average**		107.43	175.53	161.10	37.56	50.46	15.73	53.17	11.75	12.41	42
	SD		6.69	18.68	16.39	5.88	5.77	2.32	6.61	1.57	3.44	
	Range		95.33-116.43	143.86-243.38	131.25-219.05	27.89-55.22	40.36-64.18	11.29-21.20	38.02-65.82	9.21-16.19	6.98-22.60	
Todarodes sagittatus	**Average**		107.93	162.50	149.93	36.90	49.05	15.16	28.45	9.67	12.38	15
	SD		6.98	8.67	7.01	4.55	4.86	2.12	2.90	0.98	2.52	
	Range		95.94-123.27	147.15-182.38	136.93-163.52	28.82-45.73	41.18-61.12	9.41-19.50	23.35-33.54	8.14-11.64	6.47-17.12	
Todaropsis eblanae	**Average**		101.97	168.28	151.72	38.50	46.49	16.08	45.84	9.77	19.00	31
	SD		6.28	10.51	8.40	3.09	3.33	1.42	4.85	0.81	2.50	
	Range		89.78-118.93	142.86-183.58	128.44-166.67	33.78-46.11	39.18-52.24	13.78-19.69	35.48-53.33	8.26-11.65	14.75-24.17	

Table 2. Schematic chromatophore pattern of *I. coindetii*, *T. sagittatus* and *T. eblanae*. Numbers indicate rows of chromatophores in an anteroposterior axis (see Material and Methods for further details). N/A, not applicable. Abbreviations: Ven, Ventral; Dor, Dorsal; Lat, Latera; AI, Arm I; AII, Arm II; Prob, Proboscis.

Species		Head					Arm Crown			Mantle														n
		Ven	Dor			Lat	AI	AII	Prob	Ven						Dor					Lat			
		1	1	2	3	N/A	N/A	N/A	N/A	1	2	3	4	5	6	1	2	3	4	5	1	2	3	
Illex coindetii	**Average**	1.9	1.0	3.0	N/A	0.2	1.8	0.2	3.4	4.3	2.4	3.7	3.2	1.8	2.0	1.0	2.6	2.4	0.9	1.0	3.1	N/A	3.8	52
	SD	0.4	0.1	0.3	N/A	0.5	2.5	0.4	3.7	0.8	1.4	1.2	1.3	1.3	0.1	1.0	1.1	0.9	1.3	0.0	0.5	N/A	0.7	
	Range	0-2	1.0	2-4	N/A	0-2	0-10	0-1	0-16	3-6	0-6	0-6	0-5	0-4	1-2	0-3	0-5	1-4	0-4	1	2-4	N/A	3-5	
	Mode	**2**	**1**	**3**	**N/A**	**0**	**3**	**0**	**2**	**4**	**2**	**4**	**3**	**3**	**2**	**2**	**3**	**3**	**0**	**1**	**3**	**N/A**	**4**	
Todarodes sagittatus	**Average**	0	1.0	3.0	N/A	0.0	0.0	0.0	0.0	2.6	5.1	3.9	1.8	N/A	N/A	3.1	1.0	3.1	0.2	0.0	1.9	N/A	2.5	29
	SD	0	0.2	0.5	N/A	0.0	0.0	0.0	0.0	0.8	1.1	1.1	0.6	N/A	N/A	0.9	0.9	1.0	0.5	0.2	0.2	N/A	0.6	
	Range	0	0-1	1-4	N/A	0	0	0	0	2-5	3-6	2-5	0-3	N/A	N/A	2-5	0-4	2-5	0-2	0-1	1-2	N/A	1-3	
	Mode	**0**	**1**	**3**	**N/A**	**0**	**0**	**0**	**0**	**2**	**6**	**5**	**2**	**N/A**	**N/A**	**3**	**1**	**4**	**0**	**0**	**2**	**N/A**	**3**	
Todaropsis eblanae	**Average**	1.8	1.0	1.9	2.7	0.0	0.0	0.0	0.0	6.6	4.5	1.3	0.8	4.2	0.8	3.6	1.7	2.7	2.3	1.9	3.0	2.3	3.2	43
	SD	0.5	0.0	0.5	0.7	0.0	0.0	0.0	0.0	0.8	1.4	1.5	1.4	1.4	0.5	1.2	1.5	1.7	1.7	0.6	0.5	0.8	0.7	
	Range	0-2	1	0-2	0-3	0	0	0	0	5-9	1-6	0-5	0-5	0-6	0-2	1-5	0-5	0-5	0-5	1-3	2-4	1-4	2-4	
	Mode	**2**	**1**	**2**	**3**	**0**	**0**	**0**	**0**	**7**	**5**	**0**	**0**	**5**	**2**	**3**	**0**	**5**	**0**	**2**	**3**	**2**	**3**	

Table 3. Rhynchoteuthion paralarvae species according to the ratio of sucker sizes, number and arrangement of pegs of the proboscis and arm suckers. The ratio of sucker sizes is indicated only when greater than 1.

Species		Paralarval type	Ratio	Proboscis suckers			Arm suckers			n
				Internal pegs	External pegs	Free pegs	Internal pegs	External pegs	Free pegs	
Illex coindetii	Average	C	-	12.9	N/A	6.4	12.1	12.2	0.5	11
	SD			1.4	N/A	2.8	1.0	1.4	0.5	
	Range			10-14	N/A	1-12	10-14	10-14	0-1	
	Mode			14	N/A	8	12	11	0	
Todarodes sagittatus	Average	B	1.2:1	18.0	17.0	0.0	16.2	14.0	0.0	7
	SD			3.0	3.0	0.0	1.7	2.1	0.0	
	Range			12-24	12-22	0	14-19	9-17	0	
	Mode			18	14	0	16	14	0	
Todaropsis eblanae	Average	C	-	18.2	22.0	0.5	17	20.6	1.6	11
	SD			1.0	2.2	1.0	0.8	1.5	2.3	
	Range			16-24	17-27	0-3	15-18	18-23	0-8	
	Mode			18	22	0	17	20	0	

Table 4. Wild rhynchoteuthion from the NE Atlantic (most from the NW Mediterranean) identified to the species level using the identification key described here. The collecting information and the specific diagnostic characters used in the identification are shown. The measurements were performed on preserved paralarvae, so an undetermined shrinkage is expected in relation to live paralarvae. * Measurements taken from a defrosted specimen.

Species	Cruise, station and geographic coordinates	Depth (m)	Seafloor depth (m)	Date and hour	n	DML (mm)	VML (mm)	Diagnostic characters
Illex coindetii	CACO 1, st. 9, 40.42 º N 1.05 E	0-81	88	7-19-2003, 12:31	1	No data	0.97	Type C rhynchoteuthion, no photophores, only one row of pegs in proboscis suckers.
Illex coindetii	CACO 2, st. 5, 40.23º N 1.16º E	0-120	125	9-12-2003, 2:35	1	2.43	2.18	Type C rhynchoteuthion, no photophores, only one row of pegs in proboscis suckers (Fig. 4a).
Illex coindetii	CACO 2, st. 9, 40.43º N 1.06º E	0-80	88	9-12-2003, 13:10	1	2.15	2.13	Type C rhynchoteuthion, no photophores, only one row of pegs in proboscis suckers.
Illex coindetii	CACO 3, st. 4, 40.27º N 1.02º E	0-85	95	6-24-2004, 0:47	1	1.29	1.21	Type C rhynchoteuthion, no photophores, only one row of pegs in proboscis suckers.
Illex coindetii	CACO 3, st. 8, 40.38º N 1.21º E	0-100	107	6-24-2004, 12:03	2	1.06, 1.16	1.02, no data	Type C rhynchoteuthion, no photophores, only one row of pegs in proboscis suckers.
Illex coindetii	CACO 3, st. 23, 40.95º N, 1.12º E	0-65	75	6-26-2004, 00:48	1	2.02	2.06	Type C rhynchoteuthion, no photophores, only one row of pegs in proboscis suckers.
Illex coindetii	CACO 3, st. 24, 40.90º N 1.26º E	0-100	110	6-26-2004, 05:38	1	1.33	1.24	Type C rhynchoteuthion, no photophores, only one row of pegs in proboscis suckers
Todarodes sagittatus	CACO 3, st. 43, 41.49º N, 2.70º E	0-125	135	6-28-2004, 03:40	2	1.68, 2.20	1.60, 2.09	Type B rhynchoteuthion, no photophores, two rows of pegs in proboscis suckers (Fig. 4d).
Illex coindetii	CACO 3, st. 55, 41.75º N 3.50º E	0-200	765	6-29-2004, 13:47	1	2.84	3.06	Type C rhynchoteuthion, no photophores, only one row of pegs in proboscis suckers.
Todarodes sagittatus	CACO 4, st. 34, 41.11º N 2.20º E	0-200	625	7-25-2004	2	0.77, 1.03	0.94, 0.93	Type B rhynchoteuthion, no photophores, two rows of pegs in proboscis suckers.
Illex coindetii or *Todaropsis eblanae*	LLUÇ3, 4.3, 41.00 °N 1.42° E	0-186	No data	4-06-1999, 21:00	1	No data	1.97	Type C rhynchoteuthion, no photophores, proboscis suckers not visible.
Illex coindetii	FishJelly, 41.38´ N 2.21´ E	0-10	No data	10-21-2014, 11:00	1	1.03	0.94	Type C rhynchoteuthion, no photophores. Chromatophore pattern visible in this specimen and compatible with *I. coindetii* and not with *T. eblanae* (Fig. 4b-c).
Stenoteuthis pteropus	MAFIA, PEL07, 7.15 ºN 23.97 ºW	0-100	4245	4-17-2015, 23:28	1	7.71*	7.11*	Type C rhynchoteuthion, two equal-sized intestinal photophores (Fig. 4g) and an ocular photophore in each eye (Fig. 4f).

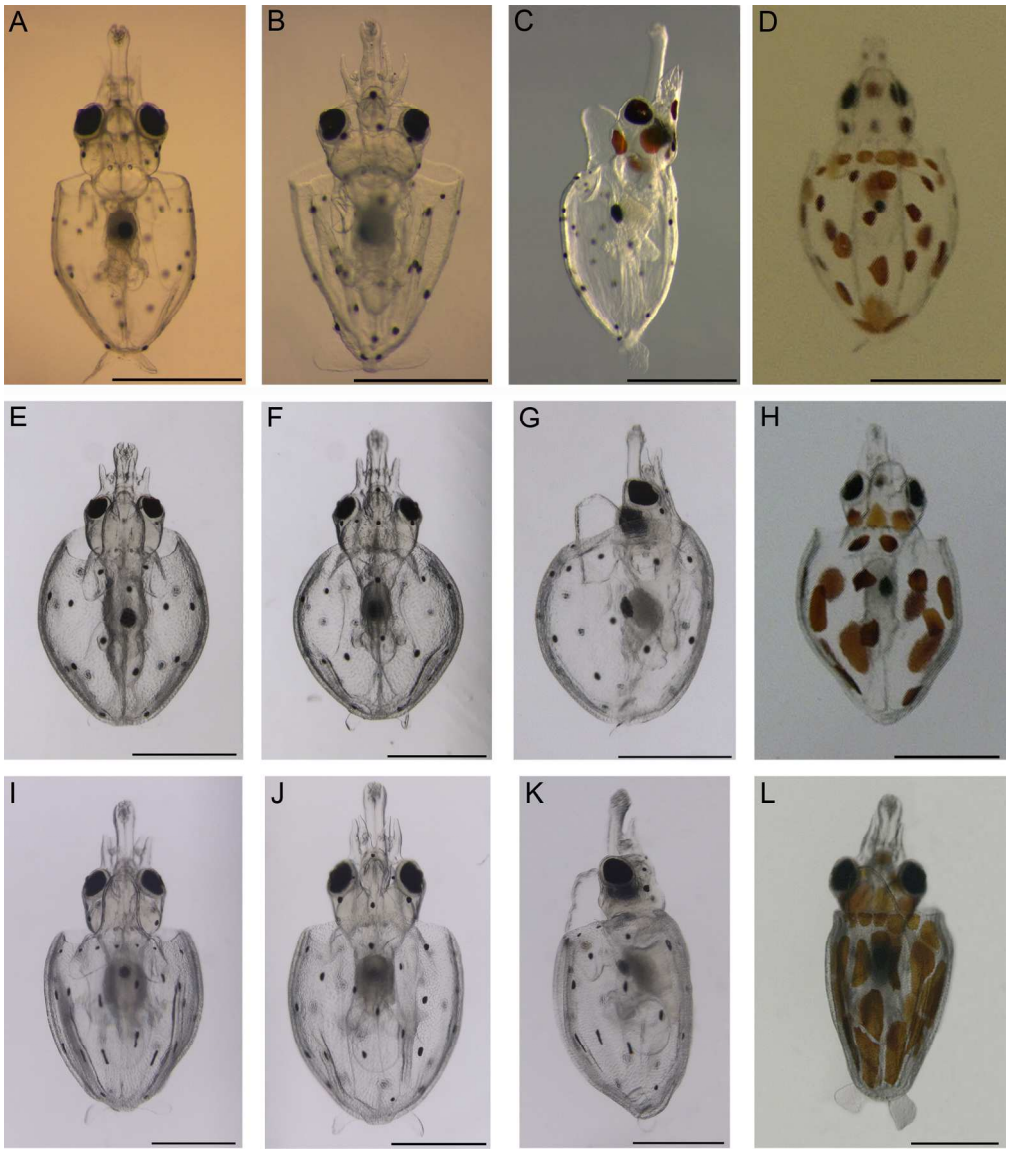

Figure 1. (a-d) Illex coindetii. a) Ventral view, aged 354 h and incubated at 17 ºC. b) Dorsal view, aged 427 h and incubated at 17 ºC. c) Lateral view, aged 262 h and incubated at 21 ºC. d) Ventral view of an individual with expanded chromatophores, aged 236 h and incubated at 17 ºC. (e-h) Todarodes sagittatus. e) Ventral view, aged 364 h and incubated at 15 ºC. f) Dorsal view, aged 358 h and incubated at 17 ºC. g) Lateral view, aged 360 h and incubated at 17 ºC. h) Ventral view of an individual with expanded chromatophores, aged 336 h and incubated at 17 ºC. (i-l) Todaropsis eblanae. i) Ventral view, aged 475 h and incubated at 17 ºC. j) Dorsal view, aged 500 h and incubated at 15 ºC. k) Lateral view, aged 498 h and incubated at 15 ºC. l) Ventral view of an individual with expanded chromatophores, aged 649 h and incubated at 15 ºC. a-c, e-g, i-k, specimens anaesthetized with ethanol, which potentially causes chromatophore contraction. d, h, l, individuals without anaesthesia. Scale bars: 1 mm.

173x197mm (300 x 300 DPI)

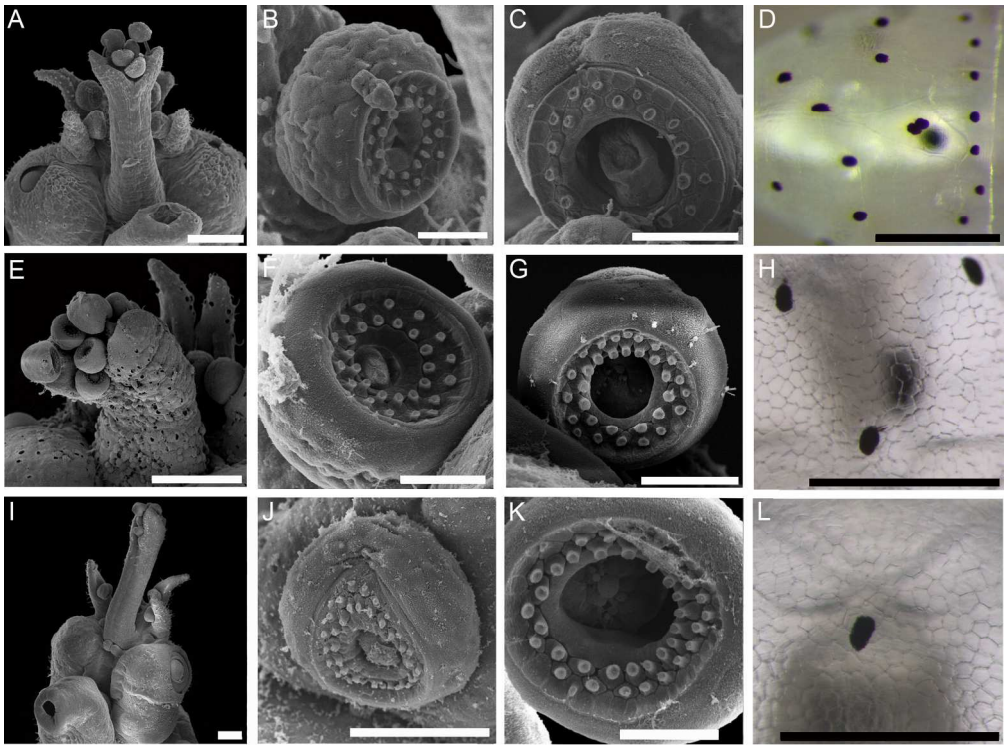

Figure 2. (a-d) Illex coindetii. a) SEM image of the ventral view of the head, aged 270 h and incubated at 17 ºC. b) SEM image of the arm I sucker, aged 270 h and incubated at 17 ºC. c) SEM image of a proboscis sucker, aged 454 h and incubated at 17 ºC. d) Detail of the ventral skin of an anaesthetized specimen, aged 329 h and incubated at 21 ºC. (e-h) Todarodes sagittatus. e) SEM image of proboscis tip, showing the differences between the lateral and medial suckers, aged 361 h and incubated at 15 ºC. f) SEM image of the left arm I sucker, aged 361 h and incubated at 15 ºC. g) SEM image of a proboscis sucker, aged 361 h and incubated at 15 ºC. h) Detail of the ventral skin of an anaesthetized specimen, aged 383 h and incubated at 15 ºC. (i-l) Todaropsis eblanae. i) SEM image of the ventrolateral view of the head of a paralarva, aged 477 h and incubated at 15 ºC, the III and IV pairs of arm stumps are visible. j) SEM image of the sucker of the left arm I, aged 475 h and incubated at 15 ºC. k) SEM image of a proboscis sucker, aged 477 h and incubated at 15 ºC. l) Detail of the ventral skin of an anaesthetized specimen, aged 498 h and incubated at 15 ºC. Scale bars: a, e, i, 100 µm; b, c, f, g, k, 20 µm; j, 50 µm; d, h, l, 0.5 mm.

193x143mm (300 x 300 DPI)

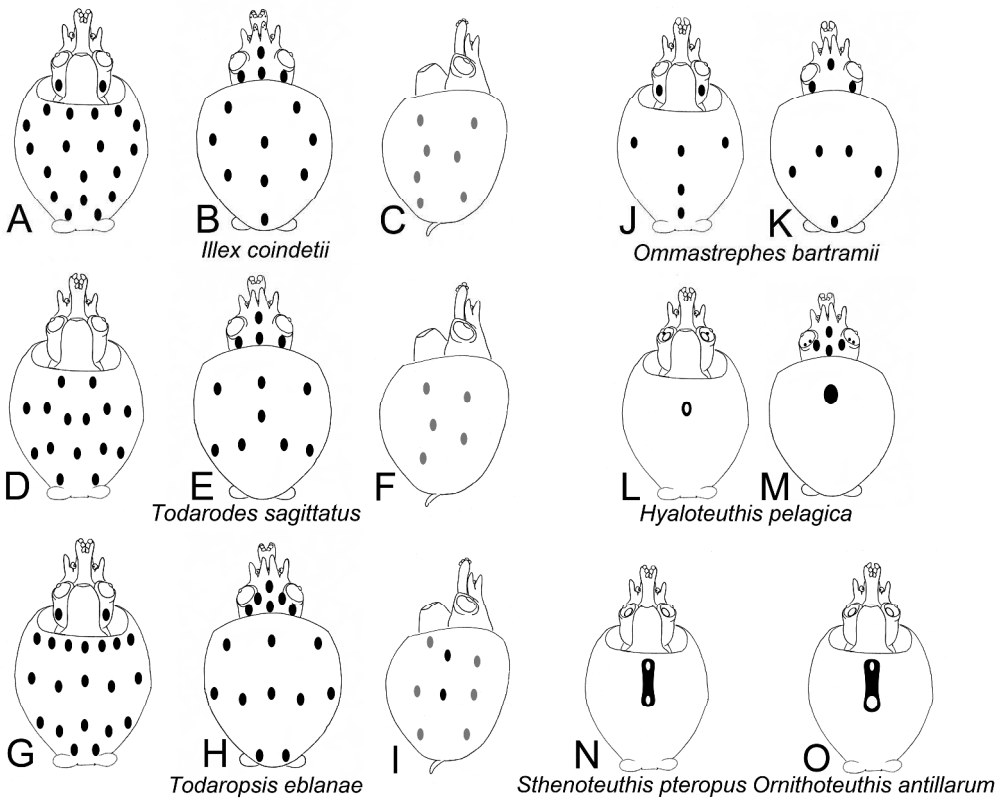

Figure 3. Schematic drawing of the chromatophore and photophore pattern of the seven North-eastern Atlantic rhynchoteuthions. (a-c) Illex coindetii. a) Ventral view. b) Dorsal view. c) Lateral view. (d-f) Todarodes sagittatus. d) Ventral view. e) Dorsal view. f) Lateral view. (g-i) Todaropsis eblanae. g) Ventral view. h) Dorsal view. i) Lateral view. (j-k) Ommastrephes bartramii. j) Ventral view. k) Dorsal view. (l-m) Hyaloteuthis pelagica. l) Ventral view. m) Dorsal view. n) Sthenoteuthis pteropus, ventral view. o) Ornithoteuthis antillarum, ventral view. Grey chromatophores of a-f depict those seen in both dorsal and ventral views. Concentric black and white circles on l-n depict ocular and intestinal photophores. Chromatophore pattern of a-f is based on the mode of the chromatophore pattern (see table 2); j-k based on Sweeney et al. (1992), Young & Hirota, (1990), Sakurai et al. (1995) and Vijai et al. (2015). Photophore and chromatophore pattern of l-m based on Harman & Young (1985) and Sweeney et al. (1992). Photophore pattern of n based on Sweeney et al. (1992), of o based on Sweeney et al (1992) and Diekmann et al. (2002). The chromatophore pattern of S. pteropus (n) and O. antillarum (o) are not known.

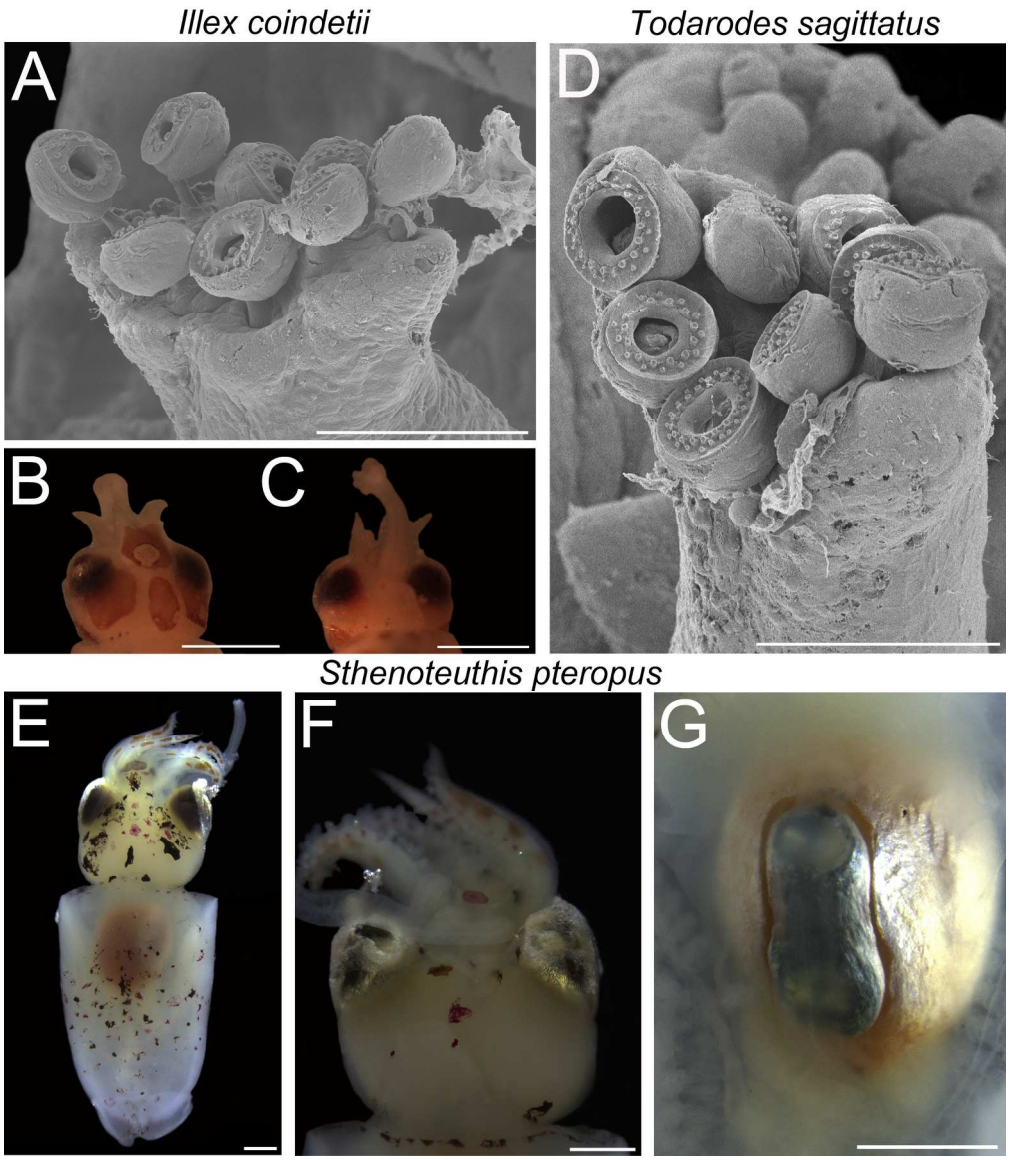

Figure 4. Main taxonomic characters used to identify wild-collected rhynchoteuthions by the dichotomous key provided here. (a-c) Illex coindetii. a) 2.4 mm DML. SEM image of the proboscis suckers, showing a single row of pegs. b-c) 1.03 mm DML. b) Dorsal view of the head showing the chromatophore pattern 1 + 3. c) Ventral view of the head showing one row of two chromatophores. (d) Todarodes sagittatus, 2.20 mm DML. SEM image of the proboscis suckers showing lateral suckers larger than the medial sucker. (e-g) Sthenoteuthis pteropus, 7.71 mm DML. e) Dorsal view of the specimen. f) Ventral view of the head showing the ocular photophores. g) Ventral view of the specimen with the mantle opened to show the two equally-sized intestinal photophores. Scale bars: a, d: 0.1 mm; b-c: 0.5 mm; e-g: 1 mm.

190x220mm (300 x 300 DPI)